ACS Medicinal Chemistry Letters

Letter

pubs.acs.org/acsmedchemlett

Comparison of the Cardiac MicroPET Images Obtained Using [^{18}F]FPTP and [^{13}N]NH_3 in Rat Myocardial Infarction Models

Dong-Yeon Kim,[†,§] Hyeon Sik Kim,[†,§] Hwa Youn Jang,[†] Ju Han Kim,[‡] Hee-Seung Bom,[†] and Jung-Joon Min*[,†]

[†]Department of Nuclear Medicine, Chonnam National University Hwasun Hospital, Hwasun, Korea

[‡]Department of Cardiology, Chonnam National University Medical School, Gwangju, Korea

Supporting Information

ABSTRACT: The short half-life of current positron emission tomography (PET) cardiac tracers limits their widespread clinical use. We previously developed a ^{18}F-labeled phosphonium cation, [^{18}F]FPTP, that demonstrated sharply defined myocardial defects in a corresponding infarcted myocardium. The aim of this study was to compare the image properties of PET scans obtained using [^{18}F]FPTP with those obtained using [^{13}N]NH_3 in rat myocardial infarction models. Perfusion abnormality was analyzed in 17 segments of polar map images. The myocardium-to-liver and myocardium-to-lung ratios of [^{18}F]FPTP were 10.48 and 2.65 times higher, respectively, than those of [^{13}N]NH_3 in images acquired 30 min after tracer injection. The myocardial defect size measured by [^{18}F]FPTP correlated more closely with the hypoperfused area measured by quantitative 2,3,5-triphenyltetrazolium chloride staining (r = 0.89, P < 0.01) than did [^{13}N]NH_3 (r = 0.84, P < 0.01). [^{18}F]FPTP might be useful as a replacement for the myocardial agent [^{13}N]NH_3 in cardiac PET/CT applications.

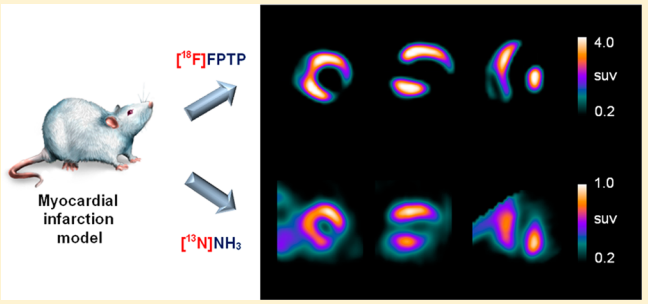

KEYWORDS: *Myocardial imaging agent, ^{18}F-labeled phosphonium salt, [^{13}N]ammonia, positron emission tomography (PET), myocardial infarction*

Nuclear medicine imaging by single photon emission computed tomography (SPECT) has played a key role in evaluating myocardial perfusion status in patients with coronary artery disease.[1] SPECT agents such as ^{99m}Tc-sestamibi, ^{99m}Tc-tetrofosmin, or ^{201}Tl are attractive surrogates for myocardial perfusion imaging (MPI) tests.[2] However, the technical limitations of SPECT imaging, such as low spatial resolution and suboptimal spread of SPECT tracers in organs adjacent to the heart, may compromise the diagnostic accuracy of SPECT for myocardial perfusion studies.[3] Positron emission tomography (PET) has several technical advantages over SPECT, such as higher spatial resolution and a standardized method to correct for photon attenuation. Owing to accurate attenuation correction, PET can provide quantitative measures of myocardial tracer uptake.[4] However, the short half-life of currently used PET tracers for MPI tests (e.g., [^{13}N]NH_3, ^{82}Rb, and [^{15}O]water) limits the widespread clinical use of PET because of the need for a nearby cyclotron or generator.[5,6] ^{18}F-labeled MPI tracers, with their longer half-life and better spatial resolution, would avoid these limitations and facilitate clinical protocols.[7,8]

To address this need, we have developed ^{18}F-labeled phosphonium cations.[9−12] Similar to SPECT tracers, such as ^{99m}Tc-sestamibi and ^{99m}Tc-tetrofosmin, phosphonium cations accumulate to higher levels in cardiomyocytes than in normal cells because of the higher mitochondrial membrane potential (MMP) in cardiomyocytes.[13−18] This type of mitochondrial voltage sensor would be useful for the detection of myocardial abnormalities because loss of MMP is an early event in cell death caused by myocardial ischemia.[14,18−20] Previously, we reported the synthesis and characterization of a novel ^{18}F-labeled phosphonium cation, (5-[^{18}F]fluoropentyl)-triphenylphosphonium salt ([^{18}F]FPTP), as a voltage sensor for myocardial imaging.[12] Biological studies, such as a biodistribution study and microPET imaging in rat models, demonstrated intense initial myocardial uptake with very rapid clearance from the background, which allowed high throughput with multiple daily studies in the clinic. Herein, we compare the image characteristics of [^{18}F]FPTP PET studies with those of the gold standard PET myocardial tracer [^{13}N]NH_3 in rat myocardial infarction (MI) models.

The structure of [^{18}F]FPTP is shown in Figure 1. The reference compound of [^{18}F]FPTP was synthesized in two procedures.[12] All compounds were analyzed by ^{1}H and ^{13}C NMR spectroscopy and FAB or ESI high-resolution mass spectroscopy to confirm the identity. The total reaction time of [^{18}F]FPTP was within 60 min, and the overall decay-corrected

Received: June 17, 2014
Accepted: September 10, 2014
Published: September 10, 2014

dx.doi.org/10.1021/ml500251z | ACS Med. Chem. Lett. 2014, 5, 1124−1128

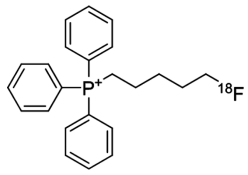

Figure 1. Structure of (5-[^{18}F]fluoropentyl)triphenylphosphonium salt ([^{18}F]FPTP).

radiochemical yield was approximately 15−20%. Radiochemical purity was >98% as measured by HPLC. [^{13}N]NH_3 was synthesized from a reduction reaction of [^{13}N]NO_x, which was produced by an $^{16}O(p, \alpha)^{13}N$ reaction, and nondecay corrected radiochemical yield was approximately 60−70%.

Static microPET images of normal rats 10, 20, and 30 min after intravenous injection of [^{18}F]FPTP or [^{13}N]NH_3 are shown in Figure 2A,B. In normal rats, microPET imaging demonstrated intense, homogeneous uptake of [^{18}F]FPTP through the myocardium and excellent myocardium-to-liver and myocardium-to-lung contrast 10 min after tracer injection. The microPET [^{13}N]NH_3 images showed higher tracer uptake by the liver than by the heart at 30 min after injection. Time activity curves (TAC) and contrast ratios between myocardium and liver or lung after tracer injection are shown in Figure 2C,D and Table 1 (n = 5, each). The TAC for [^{18}F]FPTP indicated a rapid accumulation in the myocardium (within 1−2 min) and a stable retention for at least 60 min (Figure 2C). The myocardium-to-liver ratio reached 2.0 early after [^{18}F]FPTP injection (1 min) and continued to increase until 30 min after the injection. However, the TAC of [^{13}N]NH_3 had a myocardium-to-liver ratio of 1.37 ± 0.69 (2 min after injection), and the ratio was less than 1.0 after approximately 2.5 min (Figure 2D) indicating that liver uptake of [^{13}N]NH_3 became higher than myocardium from the time point. The myocardium-to-lung ratio of [^{18}F]FPTP was over 3-fold higher than that of [^{13}N]NH_3 from 2 min after injection ($p < 0.05$). We estimated a clearance half-time of [^{18}F]FPTP and [^{13}N]NH_3 using the fitting to a single exponential as a measure of the blood clearance.[21,22] The time−activity data between image frames of 30 min were fit in the [^{18}F]FPTP and [^{13}N]NH_3 images. The clearance half-time of [^{18}F]FPTP and [^{13}N]NH_3 were 26.02 ± 6.50 and 27.72 ± 3.41 s, respectively (Figure 2E).

Images of MI models produced by acute ligation of the left coronary artery (LCA) in the short-, vertical long-, and horizontal long-axis, collected 10, 20, and 30 min after tracer injection, are shown in Figure 3A,B. Sharply defined myocardial defects were clearly detected by either tracer at the initial time point (10 min). In the repetitive imaging studies, we confirmed good image quality that allowed the defects' borders to be clearly delineated. However, the borders of the upper liver and the inferior heart overlapped in [^{13}N]NH_3 PET images, which could lead to incorrect interpretations. Subsequently, we performed 2,3,5-triphenyltetrazolium chloride (TTC) staining to measure the size of hypoperfused myocardium. The size of the area labeled with [^{18}F]FPTP or [^{13}N]NH_3 in the polar map

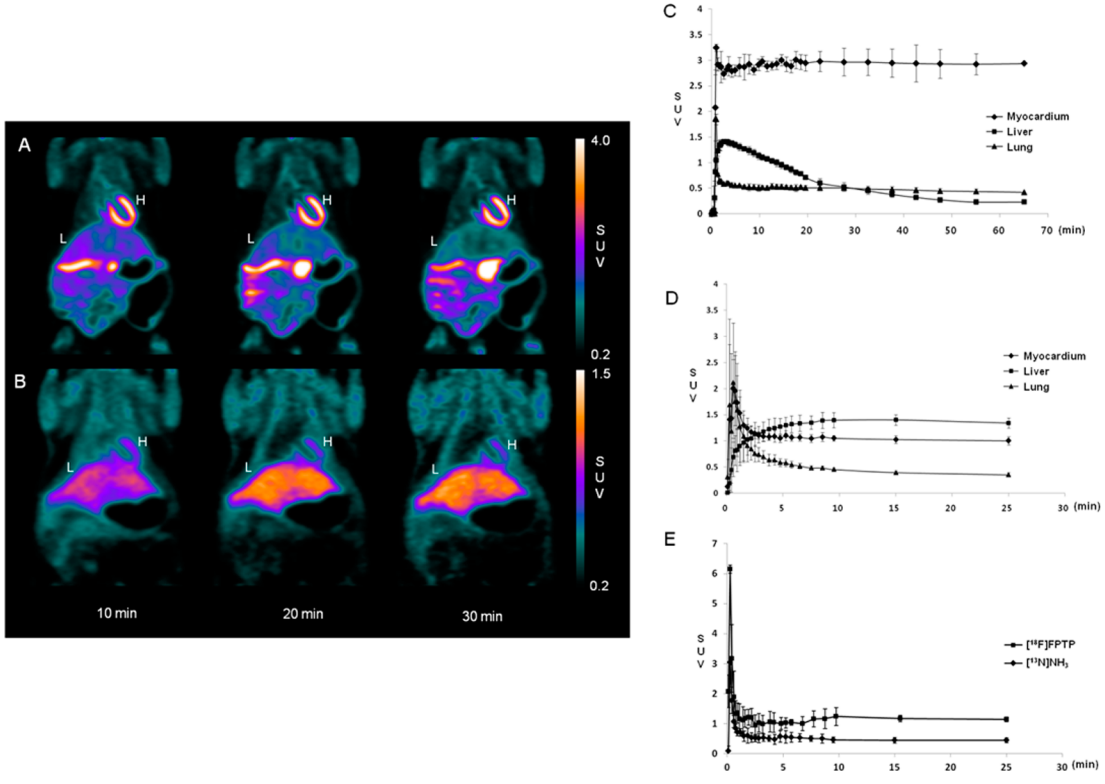

Figure 2. Coronal microPET images, time−activity curve, and blood clearance of [^{18}F]FPTP or [^{13}N]NH_3 in normal rats after intravenous injection. (A) Images acquired after injection of 37 MBq of [^{18}F]FPTP. (B) Images acquired after injection of 37 MBq of [^{13}N]NH_3. The heart was visible, with excellent heart-to-background contrast at each time point after [^{18}F]FPTP injection. H, heart; L, liver; SUV, standardized uptake value. Time−activity curves generated from dynamic microPET images using (C) [^{18}F]FPTP or (D) [^{13}N]NH_3. [^{18}F]FPTP was retained at a constant level in the myocardium but was rapidly washed out from the liver and lungs. (E) Blood clearance of [^{18}F]FPTP or [^{13}N]NH_3 in normal rats. The clearance half-time of [^{18}F]FPTP and [^{13}N]NH_3 were less than 30 s, respectively. x-axis, SUV; y-axis, time (min).

dx.doi.org/10.1021/ml500251z | ACS Med. Chem. Lett. 2014, 5, 1124−1128

Table 1. Contrast Ratios of [^{13}N]NH_3 or [^{18}F]FPTP at Each Time Point after 37 MBq Injection in Normal Rat (Myocardium-to-Liver and Myocardium-to-Lung)

	myocardium-to-liver					
	1 min	2 min	5 min	10 min	15 min	30 min
[^{18}F]FPTP	3.21 ± 0.81	2.10 ± 0.13	2.08 ± 0.17	2.58 ± 0.23	3.17 ± 0.32	5.73 ± 0.75
[^{13}N]NH_3	3.01 ± 2.38	1.37 ± 0.69	0.84 ± 0.15	0.76 ± 0.10	0.74 ± 0.09	0.75 ± 0.09
p-value	ns[a]	ns	*b*	*b*	*c*	*c*
	myocardium-to-lung					
	1 min	2 min	5 min	10 min	15 min	30 min
[^{18}F]FPTP	2.17 ± 1.25	4.51 ± 0.28	5.09 ± 0.34	5.77 ± 0.44	5.73 ± 0.75	5.95 ± 1.01
[^{13}N]NH_3	1.25 ± 0.38	1.44 ± 0.30	1.80 ± 0.17	2.31 ± 0.12	2.59 ± 0.25	2.87 ± 0.41
p-value	ns	*b*	*b*	*b*	*b*	*b*

[a]ns: not significant. [b]*$p < 0.05$. [c]**$p < 0.01$.

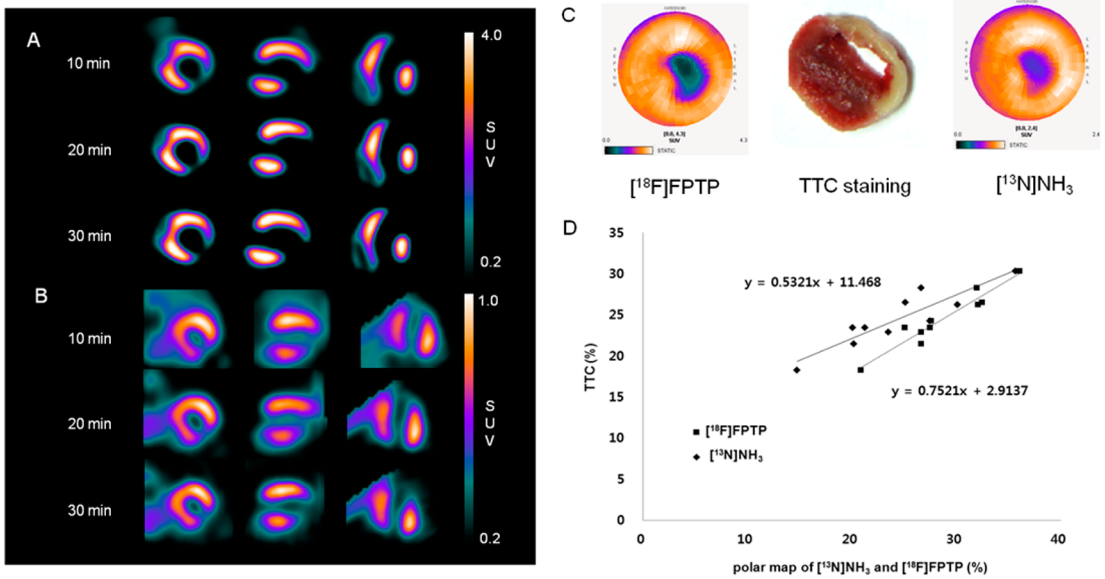

Figure 3. Short-, vertical long-, and horizontal long-axis images of (A) [^{18}F]FPTP or (B) [^{13}N]NH_3 in LCA-occluded rats. Data were collected 10, 20, and 30 min after radiotracer injection (37 MBq). Sharply defined myocardial deficits were identified with [^{13}N]NH_3 or [^{18}F]FPTP labeling in LCA-occluded rats, whereas live uptake was observed in [^{13}N]NH_3 images. (C) Polar map image of [^{18}F]FPTP or [^{13}N]NH_3 and corresponding myocardial slices stained with TTC. (D) Correlation between infarct size measured using small-animal PET and TTC staining. A threshold of 60% was set for the PET data analysis. Correlation coefficient [^{18}F]FPTP, $r = 0.89$, $P < 0.01$; [^{13}N]NH_3, $r = 0.84$, $P < 0.01$.

was also measured and was compared against the nonstained area in TTC staining ($n = 10$, each). Using polar maps with a 60% threshold, which have the best statistical significance,[12] we measured the coefficient of determination (r) for the defect size as shown by TTC staining in [^{18}F]FPTP- or [^{13}N]NH_3-labeled models. The correlation coefficient between TTC staining and labeling with [^{18}F]FPTP or [^{13}N]NH_3 was 0.89 and 0.84, respectively (Figure 3C,D). The strong correlation demonstrated that noninvasive imaging results obtained by [^{18}F]FPTP or [^{13}N]NH_3 small-animal PET can serve as a surrogate for histology to quantify the infarct size.

[^{13}N]NH_3 is generally used to quantitfy myocardial blood flow, and the uniformity and repeatability of this measurement was shown in previous studies using small animals.[23,24] High uptake of [^{13}N]NH_3 by the liver can interfere with the detection of flow abnormalities in the adjacent heart tissue. Previous studies have reported that the biodistribution of [^{13}N]NH_3 in rats was higher in the liver than in the heart.[25] [^{13}N]NH_3 (18.5 MBq, 0.5 mCi/kg) was injected into rats, and the radioactivity was measured in the heart and the liver. The initial myocardial uptake of [^{13}N]NH_3 was 2.6 ± 0.18 %ID/g at 0.2 min and decreased to 0.92 ± 0.06 %ID/g 50 min after injection. However, the initial liver uptake of [^{13}N]NH_3 was 4.83 ± 0.73 %ID/g at 0.2 min and increased to 14.4 ± 0.7 % ID/g 20 min after injection. These results indicated that the [^{13}N]NH_3 that was initially deposited in the heart was eliminated and that [^{13}N]NH_3 uptake increased in the liver over time. Furthermore, the short half-life of [^{13}N]NH_3 (9.96 min) for cardiac PET imaging limits its widespread clinical use.

[^{18}F]FPTP, which has a longer half-life (109.8 min), is a derivative of tetraphenylphosphonium cation that was originally developed for MMP measurement. The lipophilicity and delocalized positive charge enable the phosphonium cation to cross the lipid bilayer by passive diffusion and accumulate in cells in a membrane potential-dependent manner.[16,17,26] Our study demonstrated the utility of [^{18}F]FPTP as a novel myocardial perfusion agent that targets the MMP of myocardium. [^{18}F]FPTP showed homogeneously high and stable uptake properties, which provided excellent image quality when compared with [^{13}N]NH_3 in normal and MI rats. The long half-life of ^{18}F renders [^{18}F]FPTP useful for clinical PET/

dx.doi.org/10.1021/ml500251z | ACS Med. Chem. Lett. 2014, 5, 1124−1128

CT applications in patients with suspected or proven coronary artery disease.

■ ASSOCIATED CONTENT

Supporting Information

Details regarding radiochemistry, animal models, and micro-PET protocols. This material is available free of charge via the Internet at http://pubs.acs.org.

■ AUTHOR INFORMATION

Corresponding Author

*(J.-J.M.) Phone: 82-61-379-8476. Fax: 82-61-379-8455. E-mail: jjmin@jnu.ac.kr.

Author Contributions

§These authors (D.-Y.K. and H.-S.K.) contributed equally to this work. All authors have approved the final version of the manuscript.

Funding

This study was supported by a grant from the Korean Health Technology R&D Project, Ministry of Health and Welfare, Republic of Korea (HI13C0163), and was supported in part by the National Research Foundation of Korea (NRF-2012M2B2A4029856) and Chonnam National University Hospital Research Institute of Clinical Medicine (CRI 11 001).

Notes

The authors declare no competing financial interest.

■ ACKNOWLEDGMENTS

We are grateful to Ayoung Pyo for technical support of this work.

■ ABBREVIATIONS

PET, positron emission tomography; MI, myocardial infarction; MPI, myocardial perfusion imaging; SPECT, single photon emission computed tomography; MMP, mitochondrial membrane potential; TAC, time−activity curves; LCA, left coronary artery; TTC, 2,3,5-triphenyltetrazolium chloride

■ REFERENCES

(1) Camici, P. G.; Rimoldi, O. E. The clinical value of myocardial blood flow measurement. *J. Nucl. Med.* **2009**, *50*, 1076−1087.

(2) Schwaiger, M.; Melin, J. Cardiological applications of nuclear medicine. *Lancet* **1999**, *354*, 661−666.

(3) Gibbons, R. J.; Valeti, U. S.; Araoz, P. A.; Jaffe, A. S. The quantification of infarct size. *J. Am. Coll. Cardiol.* **2004**, *44*, 1533−1542.

(4) Knuuti, J.; Bengel, F. M. Positron emission tomography and molecular imaging. *Heart* **2008**, *94*, 360−367.

(5) Siegrist, P. T.; Husmann, L.; Knabenhans, M.; Gaemperli, O.; Valenta, I.; Hoefflinghaus, T.; Scheffel, H.; Stolzmann, P.; Alkadhi, H.; Kaufmann, P. A. ^{13}N-ammonia myocardial perfusion imaging with a PET/CT scanner: impact on clinical decision making and cost-effectiveness. *Eur. J. Nucl. Med. Mol. Imaging* **2008**, *35*, 889−895.

(6) Sampson, U. K.; Dorbala, S.; Limaye, A.; Kwong, R.; Di Carli, M. F. Diagnostic accuracy of rubidium-82 myocardial perfusion imaging with hybrid positron emission tomography/computed tomography in the detection of coronary artery disease. *J. Am. Coll. Cardiol.* **2007**, *49*, 1052−1058.

(7) Huisman, M. C.; Higuchi, T.; Reder, S.; Nekolla, S. G.; Poethko, T.; Wester, H. J.; Ziegler, S. I.; Casebier, D. S.; Robinson, S. P.; Schwaiger, M. Initial characterization of an ^{18}F-labeled myocardial perfusion tracer. *J. Nucl. Med.* **2008**, *49*, 630−636.

(8) Yu, M.; Guaraldi, M. T.; Mistry, M.; Kagan, M.; McDonald, J. L.; Drew, K.; Radeke, H.; Azure, M.; Purohit, A.; Casebier, D. S.; Robinson, S. P. BMS-747158-02: a novel PET myocardial perfusion imaging agent. *J. Nucl. Cardiol.* **2007**, *14*, 789−798.

(9) Kim, D. Y.; Kim, H. J.; Yu, K. H.; Min, J. J. Synthesis of ^{18}F-labeled (2-(2-fluoroethoxy)ethyl)triphenylphosphonium cation as a potential agent for myocardial imaging using positron emission tomography. *Bioorg. Med. Chem. Lett.* **2012**, *22*, 319−322.

(10) Kim, D. Y.; Kim, H. J.; Yu, K. H.; Min, J. J. Synthesis of ^{18}F-labeled (6-fluorohexyl)triphenylphosphonium cation as a potential agent for myocardial imaging using positron emission tomography. *Bioconjugate Chem.* **2012**, *23*, 431−437.

(11) Kim, D. Y.; Kim, H. J.; Yu, K. H.; Min, J. J. Synthesis of ^{18}F-labeled (2-(2-fluoroethoxy)ethyl)tris(4-methoxyphenyl)phosphonium cation as a potential agent for positron emission tomography myocardial imaging. *Nucl. Med. Biol.* **2012**, *39*, 1093−1098.

(12) Kim, D. Y.; Kim, H. S.; Le, U. N.; Jiang, S. N.; Kim, H. J.; Lee, K. C.; Woo, S. K.; Chung, J.; Bom, H. S.; Yu, K. H.; Min, J. J. Evaluation of a mitochondrial voltage sensor, ([^{18}F]fluoropentyl)-triphenylphosphonium cation, in a rat myocardial infarction model. *J. Nucl. Med.* **2012**, *53*, 1779−1785.

(13) Min, J. J.; Biswal, S.; Deroose, C.; Gambhir, S. S. Tetraphenylphosphonium as a novel molecular probe for imaging tumors. *J. Nucl. Med.* **2004**, *45*, 636−643.

(14) Madar, I.; Ravert, H.; Nelkin, B.; Abro, M.; Pomper, M.; Dannals, R.; Frost, J. J. Characterization of membrane potential-dependent uptake of the novel PET tracer ^{18}F-fluorobenzyl triphenylphosphonium cation. *Eur. J. Nucl. Med. Mol. Imaging* **2007**, *34*, 2057−2065.

(15) Madar, I.; Ravert, H.; Dipaula, A.; Du, Y.; Dannals, R. F.; Becker, L. Assessment of severity of coronary artery stenosis in a canine model using the PET agent ^{18}F-fluorobenzyl triphenyl phosphonium: comparison with ^{99m}Tc-tetrofosmin. *J. Nucl. Med.* **2007**, *48*, 1021−1030.

(16) Murphy, M. P. Selective targeting of bioactive compounds to mitochondria. *Trends. Biotechnol.* **1997**, *15*, 326−330.

(17) Fukuda, H.; Syrota, A.; Charbonneau, P.; Vallois, J.; Crouzel, M.; Prenant, C.; Sastre, J.; Crouzel, C. Use of ^{11}C-triphenylmethyl-phosphonium for the evaluation of membrane potential in the heart by positron-emission tomography. *Eur. J. Nucl. Med.* **1986**, *11*, 478−483.

(18) Higuchi, T.; Fukushima, K.; Rischpler, C.; Isoda, T.; Javadi, M. S.; Ravert, H.; Holt, D. P.; Dannals, R. F.; Madar, I.; Bengel, F. M. Stable delineation of the ischemic area by the PET perfusion tracer ^{18}F-fluorobenzyl triphenyl phosphonium after transient coronary occlusion. *J. Nucl. Med.* **2011**, *52*, 965−969.

(19) Kroemer, G. Mitochondrial control of apoptosis: an introduction. *Biochem. Biophys. Res. Commun.* **2003**, *304*, 433−435.

(20) Ross, M. F.; Kelso, G. F.; Blaikie, F. H.; James, A. M.; Cocheme, H. M.; Filipovska, A.; Da Ros, T.; Hurd, T. R.; Smith, R. A.; Murphy, M. P. Lipophilic triphenylphosphonium cations as tools in mitochondrial bioenergetics and free radical biology. *Biochemistry* **2005**, *70*, 222−230.

(21) Raffel, D. M.; Corbett, J. R.; del Rosario, R. B.; Mukhopadhyay, S. K.; Gildersleeve, D. L.; Rose, P.; Wieland, D. M. Sensitivity of [^{11}C]phenylephrine kinetics to monoamine oxidase activity in normal human heart. *J. Nucl. Med.* **1999**, *40*, 232−238.

(22) Bu, L.; Li, R.; Jin, Z.; Wen, X.; Liu, S.; Yang, B.; Shen, B.; Chen, X. Evaluation of $^{99\ m}$TcN-MPO as a new myocardial perfusion imaging agent in normal dogs and in an acute myocardial infarction canine model: comparison with $^{99\ m}$Tc-sestamibi. *Mol. Imaging Biol.* **2011**, *13*, 121−127.

(23) Lamoureux, M.; Thorn, S.; Dumouchel, T.; Renaud, J. M.; Klein, R.; Mason, S.; Lortie, M.; DaSilva, J. N.; Beanlands, R. S.; deKemp, R. A. Uniformity and repeatability of normal resting myocardial blood flow in rats using [^{13}N]ammonia and small animal PET. *Nucl. Med. Commun.* **2012**, *33*, 917−925.

(24) Slomka, P. J.; Alexanderson, E.; Jacome, R.; Jimenez, M.; Romero, E.; Meave, A.; Le Meunier, L.; Dalhbom, M.; Berman, D. S.; Germano, G.; Schelbert, H. Comparison of clinical tools for measurements of regional stress and rest myocardial blood flow

assessed with ^{13}N-ammonia PET/CT. *J. Nucl. Med.* **2012**, *53*, 171−181.
(25) Cheng, K. T. [^{13}N]Ammonia. In *Molecular Imaging and Contrast Agent Database*; National Center for Biotechnology Information: Bethesda, MD, 2004; NBK23075.
(26) Grinius, L. L.; Jasaitis, A. A.; Kadziauskas, Y. P.; Liberman, E. A.; Skulachev, V. P.; Topali, V. P.; Tsofina, L. M.; Vladimirova, M. A. Conversion of biomembrane-produced energy into electric form. I. Submitochondrial particles. *Biochim. Biophys. Acta* **1970**, *216*, 1−12.